Operation Analysis and Improvement of Impulse Current Test on High-Power DC Test Platform With SVC System

Xudong Wang, Liuwei Xu, Peng Fu, Yanan Wu, Huafeng Mao, and Jun Li

Abstract— The international thermonuclear experimental reactor poloidal field converter unit is comprised of four converter bridges, dc reactors, dc switches, etc., and most are nonstandard. To evaluate the performance of these equipments, a high-power dc test platform has been built to carry out the steady-state current test and impulse current test. The latter is significant to verify the fault suppression capability of products. The dc test platform can output the rated 400-kA impulse current. The principle design and structure of the dc test platform is introduced in this paper. The transient large current in impulse current test could cause huge impact reactive power and grid voltage sag. The impact is analyzed by theoretical calculation and simulation. A static var compensator system is added to suppress the transient effects of the reactive power. A predictive reactive power control strategy is proposed to improve the dynamic response. The comparisons with the traditional control demonstrate that the proposed control is effective in compensating impact reactive power and it also performs well on inhibiting the grid voltage sag.

Index Terms— DC test platform, impulse current, reactive power, static var compensator (SVC).

I. INTRODUCTION

THE international thermonuclear experimental reactor poloidal field converter unit (PFCU) plays a critical role in the plasma current, position, and shape control, which is an essential part in the PF coil power supply system. The PFCU is composed of 6-pulse bridges, dc reactors, external bypass, etc., and most are nonstandard [1]–[3]. To verify the performance of these equipments, a high-power dc test platform has been built to carry out temperature rise test and transient fault current test [4], [5]. The dc test platform comprises of four 6-pulse phase-controlled thyristor bridges that individually provides
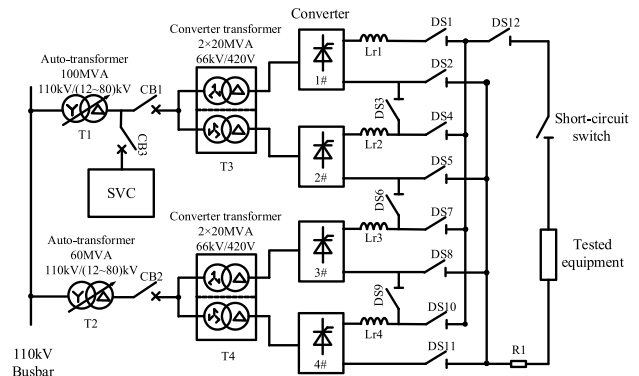
Fig. 1. Main circuit topology of the dc test platform. CB: circuit breaker, $L_{r1} - L_{r4}$: dc reactor, 1#–4#: 6-pulse bridge, short-circuit switch: circuit breaker, DS1–DS12: disconnecting switch, and R1: matched resistance.

the rated voltage 500 V and steady-state current 30 kA or transient impulse current 100 kA in 1 s. By paralleling four bridges, the dc test platform can output the rated 400-kA impulse current [6]. The impulse current test is significant to verify the fault suppression capability of external bypass and dc reactor. The impulse current test outputs transient large current under phase control technology that causes huge impact reactive power and grid voltage sag. As these will affect grid security and electrical equipment safety, it is necessary to analyze its operation and improve its performance.

This paper introduces the principle design and structure of the dc test platform in Section II. In addition, the impulse current test procedure is also discussed. In Section III, the analysis of the reactive power consumption and the voltage sag is presented. In Section IV, a static var compensator (SVC) system which is originally designed for reactive power compensation of steady-state test is added in the impulse test. A predictive reactive power control is proposed to optimize dynamic performance. In Section V, the simulations are developed in MATLAB/simulink to verify operation analysis and improvement results. Finally, the conclusion of the paper is presented.

II. SYSTEM CONFIGURATION AND OPERATION

The dc test platform system connects 110 kV substation. The short-circuit capacity at the system site of 110 kV is 1153 MVA, and the X/R is 10. The main circuit topology of the system is illustrated in Fig. 1. It is mainly composed of autotransformers, converter transformers, 6-pulse bridges,

TABLE I

MAIN PARAMETERS OF THE DC TEST PLATFORM

|	Parameters	Values	
110kV network	The short-circuit capacity, *MVA*	1153	
Auto-Transformer	Rated power, *MVA*	100	60
	Short circuit impedance(Secondary voltage 66*kV*)	9.48%	5.688%
	Rated Primary/Secondary voltage, *kV*	110/(12-80)	110/(12-80)
Converter Transformer	Rated power, *MVA*	20	
	Short circuit impedance	5.68%	
	Rated Primary/Secondary voltage, *kV*	66/0.42	
DC reactor		$50\mu H/50\mu\Omega$	

Fig. 2. Equivalent circuit of the impulse current test. (a) and (b) In the impulse current test, the converter adopts fixed firing angle. It has a fixed no-load voltage.

dc reactors, and disconnecting switches. The autotransformers have 35 tap positions in secondary side that the secondary voltage is set from 12 to 80 kV. Each 6-pulse bridge is supplied by a converter transformer, all of the which are individually shifted by ±22.5° and ±7.5° with zigzag connection in the primary side. Every 6-pusle bridge provides the rated voltage 500 V and steady-state current 30 kA or transient impulse current 100 kA in 1 s. A switch network which consists of disconnecting switch DS1–DS11 is used to configure four bridges in parallel or series. R1 is a matched resistance adjusted depending on circuit parameters and required impulse current. Because of the difference of the two autotransformer capacities, their short-circuit impedances are matched to balance the output power on both sides. The main parameters of the dc test platform are listed in Table I [6].

As the large and rapid rise impulse current is required, open-loop control with quick response is applied in the impulse test. First, according to the required impulse current, the corresponding firing angle is figured out. The no-load voltage in converter is established. Second, the short-circuit switch is closed to output impulse current. Finally, when the output current reaches the required value, the system is taken into quit process, which converters are operated in inverter mode to decline the impulse current and absorb the energy stored in the dc reactors.

To output a large impulse current, the bridges are set in parallel by configuring the switch network. The equivalent circuit of four 6-pusle bridges in parallel is shown in Fig. 2(a). The 6-pusle bridges can be equivalent to no-load voltages $U_1 - U_4$ with internal resistances $R_{S1} - R_{S4}$. The internal resistance is mainly composed of short-circuit impedance of autotransformer, converter transformer, and 110-kV power grid, and equivalent impedance of ac busbar between converter transformer and bridge. L_d is equivalent inductance of dc busbar, R_d is equivalent resistance of dc busbar, and L_r is inductance of dc reactor.

Because, four converter transformers are designed and manufactured consistently and the short-circuit impedance of two autotransformers is matched, the internal resistances
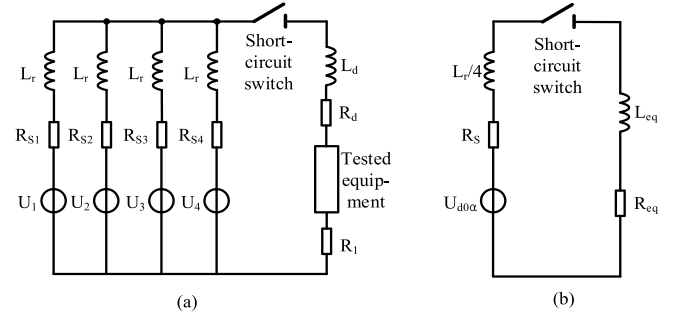
$R_{S1} - R_{S4}$ are approximately equal. The equivalent circuit is simplified, as shown in Fig. 2(b). L_{eq} is a sum of L_d and equivalent inductance of tested equipment, and R_{eq} is a sum of R_d, R_1 and equivalent resistance of tested equipment. So far, the system is simplified to be a first-order circuit with zero-state response. According to the main circuit topology, the system total leakage reactance is listed in the following:

$$X_s = X_L + \frac{X_{\text{AT}}}{2} + \frac{X_{\text{CT}}}{4} + \frac{X_{\text{AB}}}{4} \qquad (1)$$

where X_L is the power grid reactance; X_{AT} is the reactance of autotransformer; X_{CT} is the reactance of converter transformer; and X_{AB} is the reactance of ac busbar between converter transformer and bridge.

It is important to note that all of these parameters are converted to the converter transformer secondary side. The equivalent resistance R_S is obtained as $R_s = 3X_s/\pi$.

According to the Kirchhoff's law, (2) is obtained

$$U_{d0}\cos\alpha - R_s i_d - \frac{L_r}{4}\frac{di_d}{dt} = R_{\text{eq}} + L_{\text{eq}}\frac{di_d}{dt} \qquad (2)$$

where α is converter firing angle; U_{d0} is the no-load voltage is $U_{d0} = 1.35U_2$; U_2 is secondary line voltage of converter transformer; and i_d is dc output current. The i_d could be figured out by (2)

$$i_d = \frac{U_{d0}\cos\alpha}{R_s + R_{\text{eq}}}(1 - e^{-t/\tau}) = i_{d0}(1 - e^{-t/\tau}) \qquad (3)$$

where $\tau = (L_r/4 + L_{\text{eq}}/R_s + R_{\text{eq}})$.

Combined with the characteristics of the test platform, an equivalent circuit of the impulse current test is established. The calculation is greatly simplified under the equivalent first-order circuit. The analysis of the equivalent circuit laid the foundation for reactive power and grid voltage sag analysis in the following chapters.

III. OPERATION ANALYSIS OF THE IMPULSE CURRENT TEST

Due to the huge impact reactive power in the impulse current test, it is necessary to analyze its effects on the power grid and dc test platform. There is a SVC system connected in the 100-MVA autotransformer T1 secondary. If the two autotransformers are loaded simultaneously, only the T1 is compensated with SVC system, which makes the current of the bridge arms unequal and the current sharing
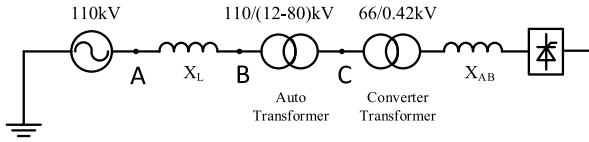
Fig. 3. System schematic.

Fig. 4. Fundamental vector diagram.

coefficient lower. As the platform is utilized as modular structure, the analytical method and process is similar for two or four bridges in parallel. In order to demonstrate the improvement of SVC system, this paper mainly presents an analysis of one autotransformer with two bridges in parallel. The method could be extended depending on the modular structure.

As the 110-kV grid is an experimental dedicated power grid, the system could be equivalent to a single access limited power supply system. The system schematic is shown in Fig. 3.

Where node A is the ideal 110-kV grid with system reactance X_L; node B is connecting 110 kV substation and the dc test platform system; and node C is linking autotransformer with converter transformer.

The system total leakage reactance with two bridges is a little different to (1) with four bridges

$$X_s = X_L + X_{AT} + \frac{X_{CT}}{2} + \frac{X_{AB}}{2}. \tag{4}$$

Based on the balance principle of active power in ac/dc power system, the fundamental active power $P_{A(1)}$ in grid equals output power P_d in dc side

$$P_{A(1)} = P_d = U_d I_d = U_{d0} I_d \frac{\cos \alpha + \cos(\alpha + \gamma)}{2}. \tag{5}$$

The line current i_L could be Fourier decomposed into fundamental active component $I_{LP(1)}$, fundamental reactive component $I_{LQ(1)}$, and high-order harmonics. Considering the firing angle α and overlap angle γ, the Fourier decomposition results are as follows:

$$i_L = \sqrt{2} I_{LP(1)} \cos \theta + \sqrt{2} I_{LQ(1)} \sin \theta$$
$$+ \sum_{5}^{n} (a_n \cos n\theta + b_n \sin n\theta) \tag{6}$$

where the fundamental active component $I_{LP(1)}$

$$I_{LP(1)} = \frac{\sqrt{6}}{2\pi} I_d [\cos \alpha + \cos (\alpha + \gamma)].$$

The fundamental reactive component $I_{LQ(1)}$

$$I_{LQ(1)} = \frac{\sqrt{6}}{4\pi} I_d \frac{\sin (2\alpha + 2\gamma) - \sin 2\alpha - 2\gamma}{\cos \alpha - \cos (\alpha + \gamma)}.$$

According to the fundamental active component $I_{LP(1)}$ and reactive component $I_{LQ(1)}$, the ratio of fundamental reactive and active power in node A is shown in the following:

$$\frac{Q_{A(1)}}{P_{A(1)}} = \frac{2\gamma + \sin 2\alpha - \sin(2\alpha + 2\gamma)}{2[\cos \alpha - \cos(\alpha + \gamma)][\cos \alpha + \cos(\alpha + \gamma)]}. \tag{7}$$
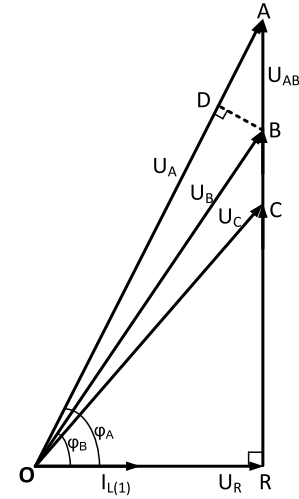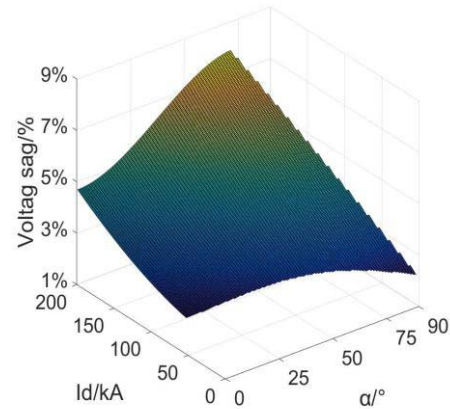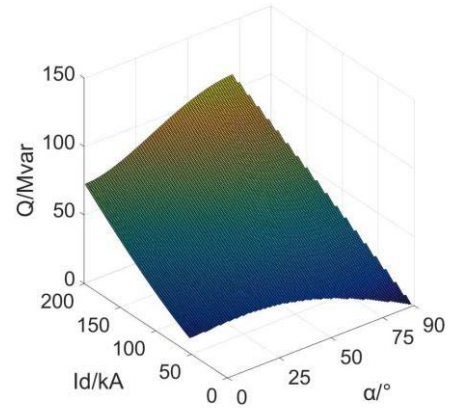

Fig. 5. Reactive power consumption and grid voltage sag at 110 kV side.

The fundamental reactive power $Q_{A(1)}$ could be expressed by (5)–(7), as shown in the following:

$$Q_{A(1)} = \frac{2\gamma + \sin 2\alpha - \sin(2\alpha + 2\gamma)}{4[\cos \alpha - \cos(\alpha + \gamma)]} U_{d0} I_d. \tag{8}$$

From (7), the displacement factor angle $\varphi_A = \arctan(Q_{A(1)}/P_{A(1)})$. By voltage vector method, all nodes voltage and displacement factor could be deduced. According to voltage balance equation, fundamental vector diagram is
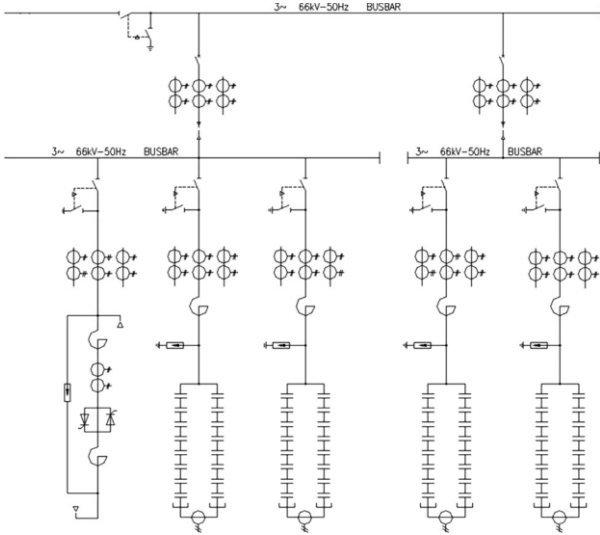
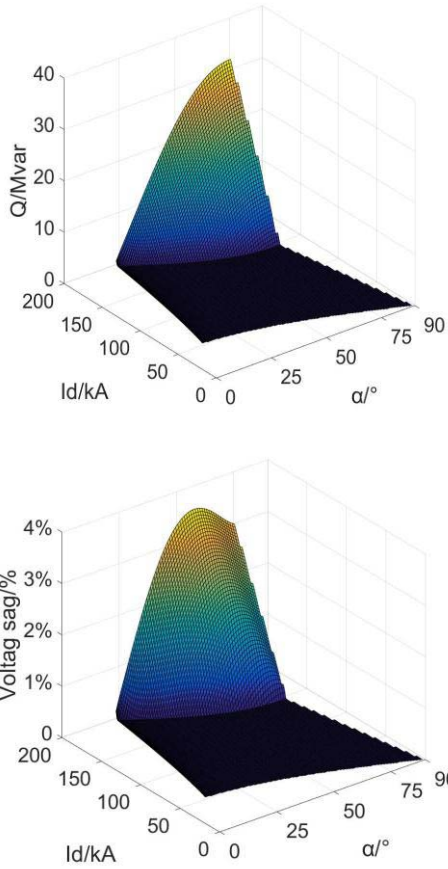Fig. 6.   Electrical schematic of SVC system.

Fig. 7.   Reactive power consumption and grid voltage sag at 110 kV side.

illustrated in Fig. 4. And the relationship of each vector is shown in the following:

$$\begin{cases} U_A^2 = U_B^2 + U_{\mathrm{AB}}^2 - 2U_B U_{\mathrm{AB}} \cos(90° + \varphi_B) \\ U_B \cos \varphi_B = U_A \cos \varphi_A \end{cases} \quad (9)$$

where the grid reactance voltage drop: $U_{\mathrm{AB}} = I_{LQ(1)} X_L$.

And also depending on the balance principle of active power in ac/dc power system, the reactive power in node B is
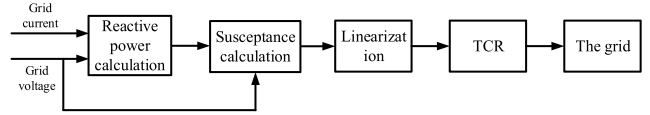

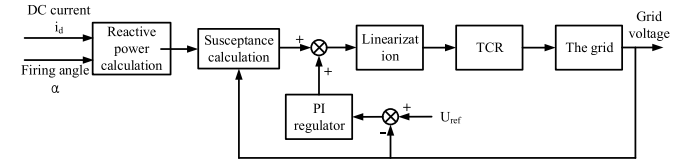Fig. 8.   Open-loop control block diagram of SVC system.

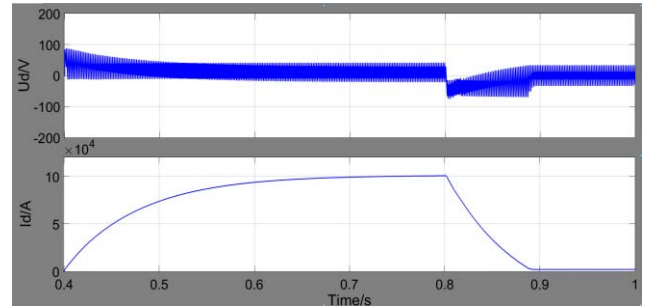Fig. 9.   Predictive reactive power control block diagram of SVC system.

Fig. 10.   DC output voltage and current.

calculated as

$$Q_{B(1)} = P_d \tan \varphi_B. \quad (10)$$

The reactive power consumption and grid voltage sag are shown in Fig. 5, respectively. With the increase of the firing angle α and dc current, the system consumes the higher reactive power. Obviously, the voltage sag caused by the reactive power has the same variation trend. Under the highest 200-kA impulse current by two bridges in parallel, the system consumes about 120-Mvar reactive power with 8% gird voltage sag.

IV.   IMPROVEMENT OF THE IMPULSE CURRENT TEST

As it is analyzed above, the impulse current test will cause high impact reactive power and grid voltage sag. It is necessary to improve and optimize the test. A SVC system connected in 66-kV busbar of T1 secondary side has been constructed. It has been confirmed to perform well in reactive power compensation, harmonic suppression, and voltage maintenance for integration test on the PFCU prototype test platform with fast response [7]–[9]. The SVC system is considered to be introduced in the impulse current test to suppress the impact.

The SVC system consists of thyristor controlled reactors (TCR) and fixed capacitors, with the rated fundamental compensation capacity 83.2 Mvar under 66-kV voltage level. Four fixed harmonic filters tuned to the 3rd, 5th, 7th, and 11th harmonics of 50 Hz are set. Its electrical schematic is shown in Fig. 6 and parameter configuration is listed in Table II. The compensation capacity provided by the SVC system is proportional to the square of the bus voltage: $Q_{\mathrm{svc}} = 83.2(U_C/66)^2$ Mvar. U_c is the bus voltage at the point of common coupling (PCC).
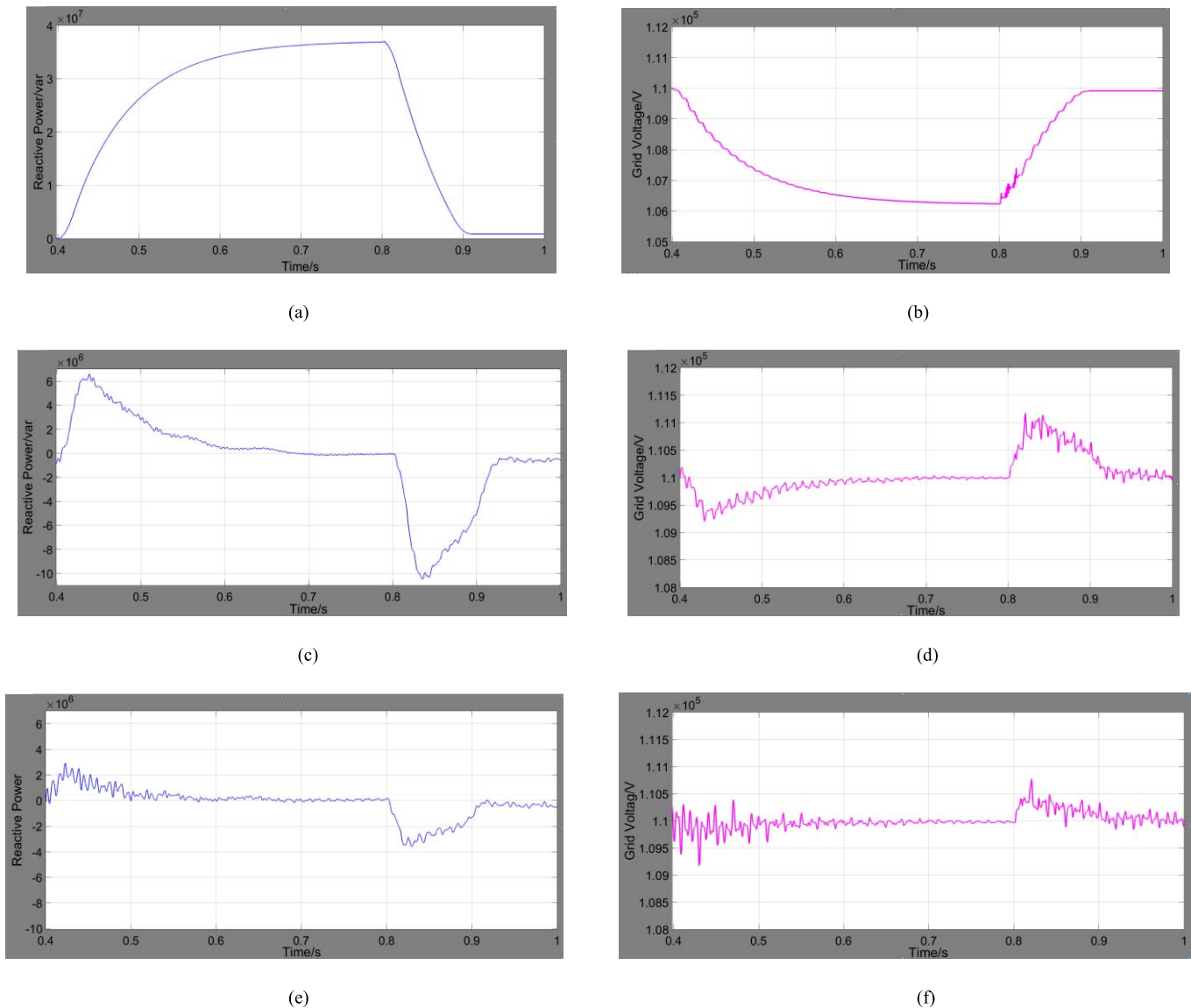
Fig. 11. Comparisons of simulation results. Single test. (a) Reactive power consumption at 46 kV side. (b) Grid voltage at 110 kV side. United test under open-loop control. (c) Reactive power consumption at 46 kV side. (d) Grid voltage at 110 kV side. United test under predictive control. (e) Reactive power consumption at 46 kV side. (f) Grid voltage at 110 kV side.

As the PCC in the autotransformer T1 secondary side, the impulse test with SVC system can only be operated in single autotransformer with two 6-pulse bridges. However, due to its modular design, the theoretical method and simulation analysis of the united test can be developed for multiple parallel bridges. It can provide theoretical basis and verification for the improvement of dc test platform and the capacity expansion of SVC system.

In the united test, as there are three unknown variables that are reactive power consumption, reactive power compensation, and grid voltage sag, it cannot calculate the variables by the voltage vector method directly. The balance of the three variables could be figured out by iterative computation in MATLAB or other computing softwares. Setting the iteration criterion: $\Delta Q_{(1)} = |Q_{(1)}(k+1)| - |Q_{(1)}(k)| < 0.5$ Mvar, the reactive power consumption and the grid voltage sag are shown in Fig. 7, respectively. The capacity of the existing

SVC system is satisfied to compensate the reactive power consumption of almost 200-kA impulse current and the grid voltage sag is decreased from 8% to 3.5%. The SVC system is effective in compensating reactive power and inhibiting the power grid voltage sag.

Under limited condition of $R_{eq} = 0.1$ mΩ in dc side, the 110 kV grid voltage slightly exceeds the requirement of 3% voltage fluctuation in Chinese National Standard "GB/T 12326-2008 power quality voltage fluctuation and flicker." By the iteration calculation, when the capacity of SVC system is extended to 90 Mvar, it can satisfy the compensation requirement of the impulse current 200 kA.

Due to the high rising output current and impact reactive power in the test, the response speed of SVC system is a primary factor to be considered. The open-loop control is now used in the united test, which is mainly applied to load compensation with simple control strategy, quick response,

TABLE II
SVC SYSTEM PARAMETER CONFIGURATION

Parameter	TCR	Filter Circuit			
Harmonic Order		3	5	7	11
Reactive Power, *Mvar*	83.208	12.888	23.856	23.376	23.088
Inductance, *mH*	2×104	137.44	24.74	12.62	5.11
Capacitance, *uF*		8.357	16.714	16.714	16.714
Quality Factor		93	107	65	38

and reliable operation. The control block diagram is shown in Fig. 8 [9], [10].

However, Steinmetz compensation principle used in open-loop control will consume sampling period 20 ms. In addition, dead time and trigger delay both increase response times in thyristor control of TCR circuit. The response speed of the open-loop control could not be sufficient to meet the fast increase of the reactive power demand. As the test platform adopts the fixed firing angle and the reactive power is calculated simply and exactly, this paper presents a predictive reactive power method. The predictive reactive power is calculated depending on the firing angle α and dc output current i_d, which is used as feedforward compensation. And the grid voltage is introduced as feedback to correct compensation error caused by the reactive power calculation. The control block diagram is shown in Fig. 9 [10]–[12].

The predictive control combines the advantages of open-loop and closed-loop control, the real-time detection of reactive power is canceled and the negative feedback of grid voltage stabilizes the grid voltage. Compared with the traditional open-loop control, the proposed predictive control consumes less time with higher accuracy.

V. COMPARISON AND ANALYSIS OF SIMULATIONS

In order to evaluate and assess the theoretical analysis and transient performance of the dc test platform with SVC system and to validate the advantages of the proposed predictive reactive power control, the relevant simulations have been developed based on MATLAB/simulink. The tap of the 100-MVA autotransformer T1 is set in 46 kV, and the impulse current is set at 100 kA in 400 ms.

At the time 0.4 s, closing short-circuit breaker, the platform starts to output impulse current. Then 400 ms later taking the firing angle in inverted mode, the platform entries quit status. The dc output voltage and current are shown in Fig. 10.

The reactive power consumption and grid voltage of the single test without SVC system are shown in Fig. 11(a) and (b), respectively. The reactive power consumption is about 36 Mvar and the grid voltage is about 106.2 kV. The variation trend of the reactive power consumption and grid voltage follows the dc output current. The simulation results are consistent with the theoretical calculation.

The united test simulation results with open-loop control are shown in Fig. 11(c) and (d). Consistent with the theory analysis, the delay time of open-loop control is so long that it is unsatisfied with the response speed. The reactive power has an over 6-Mvar peak and a 10 Mvar over compensation appears on quit mode. And also the grid voltage has a transient fluctuate. Due to its slow response time, there is an over voltage in quit mode. As the impulse current increases, these phenomena will become more and more serious.

Fig. 11(e) and (f) shows the simulation results of the united test under predictive control. The response time is up to about 10 ms faster. (The response time starts from the system start to the first peak of the reactive power.) The peak of reactive power reduces to 2.8 Mvar and the over compensation has lowered to 4 Mvar. Both of them are improved about 60%. The transient fluctuate of voltage and over voltage is suppressed significantly.

VI. CONCLUSION

This paper introduced the configuration and operation of dc test platform. The simplified equivalent circuit of the impulse current test is also presented. The reactive power consumption and grid voltage sag is analyzed. To improve the test performance, a SVC system is introduced to compensate the reactive power and stabilize the grid voltage. A predictive reactive power control strategy is proposed to improve its dynamic response. The simulation results of the proposed control are compared with the traditional open-loop control that the effectiveness of the proposed control is evaluated to reduce reactive power transient peak with lower voltage transient fluctuate. This paper also provided a design reference for the capacity expansion of the SVC system to meet reactive power compensation for the higher impulse current test in the future.

REFERENCES

[1] J. Tao *et al.*, "ITER coil power supply and distribution system," in *Proc. 24th IEEE/NPSS Symp. Fusion Eng. (SOFE)*, Jun. 2011, pp. 1–8.
[2] P. Fu *et al.*, "Review and analysis of the AC/DC converter of ITER coil power supply," in *Proc. 25th Annu. IEEE Appl. Power Electron. Conf. Expo. (APEC)*, Feb. 2010, pp. 1810–1816.
[3] P. Fu *et al.*, "Preliminary design of the poloidal field AC/DC converter system for the ITER coil power supply," *Fusion Sci. Technol.*, vol. 64, no. 4, pp. 741–747, 2013.
[4] Z. Song *et al.*, "Prototype design and test of ITER PF converter unit," *IEEE Trans. Plasma Sci.*, vol. 44, no. 9, pp. 1677–1683, Sep. 2016.
[5] P. Wang, Z. Song, and C. Li, "Prototype design of external bypass for ITER poloidal field converter," *IEEE Trans. Plasma Sci.*, vol. 44, no. 9, pp. 1525–1528, Sep. 2016.
[6] X. Zhang, P. Fu, G. Gao, L. Xu, and Z. Song, "Transient fault current test for ITER DC reactor on dc test platform in ASIPP," *J. Fusion Energy*, vol. 33, no. 5, pp. 607–611, 2014.
[7] A. D. Mankani *et al.*, "The ITER reactive power compensation and harmonic filtering (RPC & HF) system: Stability & performance," in *Proc. 24th IEEE/NPSS Symp. Fusion Eng. (SOFE)*, Jun. 2011, pp. 43–48.

[8] L. Xu *et al.*, "The reactive power compensation and harmonic filtering and the over-voltage analysis of the ITER power supply system," in *Proc. 25th Annu. IEEE Appl. Power Electron. Conf. Expo. (APEC)*, Feb. 2010, pp. 1622–1626.

[9] S. Zhicai, F. Peng, and X. Liuwei, "Dynamic performance of the ITER reactive power compensation system," *Plasma Sci. Technol.*, vol. 13, no. 5, pp. 637–640, 2011.

[10] Y. Wu *et al.*, "Optimization for Tokamak reactive power compensation and filtering system," *J. Fusion Energy*, vol. 34, no. 1, pp. 54–61, 2015.

[11] C. Finotti, E. Gaio, I. Song, J. Tao, and I. Benfatto, "Improvement of the dynamic response of the ITER reactive power compensation system," *Fusion Eng. Des.*, vols. 98–99, pp. 1058–1062, Oct. 2015.

[12] C. W. Taylor, "Static VAr compensator models for power flow and dynamic performance simulation," *IEEE Trans. Power Syst.*, vol. 9, no. 1, pp. 229–240, Feb. 1994.

Peng Fu was born in Hubei, China, in 1962. He received the B.S. degree in electrical engineering from the Huazhong University of Science and Technology, Wuhan, China, in 1985, and the M.S. and Ph.D. degrees in electrical engineering from the Chinese Academy of Sciences, Hefei, China, in 1990 and 1997, respectively.

He is currently a Professor and a Manager of the International Thermonuclear Experimental Reactor Project with the Institute of Plasma Physics, Chinese Academy of Sciences. His current research interests include power supplies and their control systems of fusion devices.

Xudong Wang was born in Anhui, China, in 1988. He received the B.S. degree in electrical engineering and the M.S. degree in power electronics and power drives from Beijing Jiaotong University, Beijing, China, in 2010 and 2012, respectively. He is currently pursuing the Ph.D. degree in nuclear energy science and engineering with the University of Science and Technology of China, Hefei, China.

His current research interests include operation analysis of magnetic coil power supply and reactive power compensation system.

Yanan Wu was born in Anhui, China, in 1986. He received the B.S. degree in automation from the South-Central University For Nationalities, Wuhan, China, in 2009, and the Ph.D. degree in nuclear energy science and engineering from the Institute of Plasma Physics, Chinese Academy of Science, Hefei, China, in 2015.

His current research interests include compatibility on fusion device power supply and reactive power compensation system with the grid.

Huafeng Mao was born in Anhui, China, in 1976. He received the B.S. degree in electrical engineering from the Huazhong University of Science and Technology, Wuhan, China, in 2011.

His current research interests include the testing of reactive power compensation and harmonic filter.

Liuwei Xu was born in Henan, China, in 1967. He received the B.S. degree in electrical engineering from the Hefei University of Technology, Hefei, China, in 1989, and the M.S. degree in nuclear energy science and engineering from the Chinese Academy of Sciences, Hefei, in 1999.

He is currently a Professor of the International Thermonuclear Experimental Reactor Project with the Institute of Plasma Physics, Chinese Academy of Sciences. His current research interests include magnet power supplies and reactive power compensation systems of fusion devices.
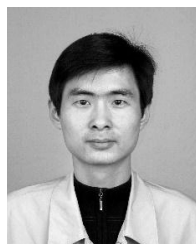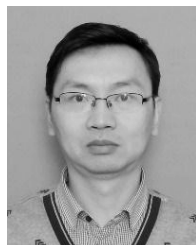
Jun Li was born in Anhui, China, in 1980. He received the B.S. degree in automation from the Hefei University of Technology, Hefei, China, in 2004, where he is currently pursuing the M.S. degree in electrical engineering.

His current research interests include thyristor controlled reactor and hybrid active power filter of fusion device.